Research Article

Received: 24 October 2013 Revised: 25 January 2014 Accepted article published: 5 February 2014 Published online in Wiley Online Library: 12 March 2014

(wileyonlinelibrary.com) DOI 10.1002/jctb.4348

A framework to predict and experimentally evaluate polymer–solute thermodynamic affinity for two-phase partitioning bioreactor (TPPB) applications

Stuart L. Bacon, J. Scott Parent and Andrew J. Daugulis*

ABSTRACT

BACKGROUND: Selection of a polymer for two-phase partitioning bioreactor (TPPB) applications has previously been limited to heuristic approaches. However, recent interest has focused on first principles' selection methods based on polymer crystallinity, glass transition temperature and polymer–solute thermodynamic affinity. In this work, a framework is proposed to evaluate and predict polymer–solute thermodynamic affinity via the polymer-phase activity coefficient.

RESULTS: Polymer screening via thermodynamic affinity was shown to be most effective at very dilute concentrations, where partition coefficients can be estimated using infinite dilution activity coefficients. In the absence of published values, UNIFAC-vdW-FV or Flory–Huggins based activity models can provide very good predictions for the polymer-phase activity coefficient, significantly improving upon previous approaches using Hildebrand and Hansen solubility parameter differences. For non-dilute systems, however, the activity models failed to consider the full effects of concentration on partition coefficient. Additionally, a reduction in polymer molecular weight resulted in improved partition coefficients, a phenomena well described by the activity models.

CONCLUSION: Predicting and experimentally quantifying polymer–solute thermodynamic affinity at very dilute concentrations will aid future attempts at TPPB polymer selection. Furthermore, experimental partition coefficient data at a range of operational concentrations will indicate how TPPB effectiveness will change throughout the fermentation course. Finally, reduction of polymer molecular weight to improve solute partitioning should be investigated further for a range of polymers.

Supporting information may be found in the online version of this article.

Keywords: polymer solution thermodynamics; TPPB; partitioning bioreactor; liquid–liquid extraction; solubility parameter; UNIFAC-vdW-FV; activity model

INTRODUCTION

Bioprocess productivity is commonly hindered by substrate and/or product inhibition. Benefits have been previously demonstrated by introducing a non-aqueous phase (NAP), used to sequester the toxic target molecule and lower its aqueous concentration to sub-inhibitory levels. This technology platform, commonly referred to as a two-phase partitioning bioreactor (TPPB), has been successfully demonstrated with a variety of NAPs including small molecule solvents,[1,2] viscoelastic oligomeric liquids (polypropylene glycol, silicone oil)[3–6] and solid co-polymer beads.[7–11] In addition to their need to be non-bioavailable and biocompatible, NAPs are screened based on substrate/product affinity *via* the partition coefficient.[12] Previous work has established a predictive screening program to rank liquid solvents based on solute affinity using the UNIFAC group contribution activity model.[13] Polymers, on the other hand, have been limited to selection through heuristic methods, prompting recent efforts to investigate first principles approaches to screening polymers on the basis of crystallinity, glass transition temperature (T_g) and thermodynamic affinity.[9,14] To fully realize the benefits of using polymers in TPPBs,[5,15] the present study provides the required framework to rationally select and evaluate a polymer based on its thermodynamic affinity for the target substrate and/or product.

Quantifying polymer–solute interactions can be achieved by finding an expression for the Gibbs free energy of mixing. Favorable polymer–solute affinity is characterized by a negative Gibbs free-energy of mixing, ΔG_M, which can be related to the enthalpy and entropy of mixing, ΔH_M and ΔS_M, by Equation (1):

$$\Delta G_M = \Delta H_M - T\Delta S_M \quad (1)$$

* *Correspondence to: Andrew J. Daugulis, Department of Chemical Engineering, Dupuis Hall. 19 Division St, Queen's University, Kingston, Ontario, Canada K7L 3N6. Email: andrew.daugulis@chee.queensu.ca*

Department of Chemical Engineering, Dupuis Hall. 19 Division St, Queen's University, Kingston, Ontario, Canada K7L 3N6.

The Flory–Huggins solution theory is the most widely used thermodynamic framework for quantifying the enthalpic and entropic contributions to the Gibbs free energy of mixing, ΔG_M.[16] Other contributions to polymer–solute mixing which could not be directly attributed as being purely enthalpic (ΔH_M) or entropic (ΔS_M) such as the free-volume effect, were later discovered.[17] Therefore, we are proposing a shift in the discussion of polymer–solute affinity from using the enthalpy and entropy of mixing to more quantifiable and conceptually available contributions. They include: (1) the combinatorial entropy of mixing; (2) intermolecular interactions between solute and polymer molecules; and (3) the free volume effect.[17,18] These three main contributions describe polymer–solute affinity by contributing to ΔS_M, ΔH_M or both.

A very thorough description of these three contributions has been provided by Patterson,[18] briefly reviewed here with respect to their overall contribution to ΔG_M. The combinatorial entropy of mixing, ΔS_M^{comb}, results from increases in positional disorder/randomness through mixing, that is, an increase in the number of possible molecular configurations from mixing two pure substances. Combinatorial entropy is always positive and is a main component of the overall entropy of mixing, ΔS_M, from Equation (1). Therefore, greater combinatorial entropy will result in more energetically favorable mixing by reducing ΔG_M. An important contribution to ΔS_M which is not included in ΔS_M^{comb} is the entropic contribution from the conformational changes associated with polymer chains unfolding.[19] This contribution is particularly significant when polymer–solute mixing induces the melting of crystals in semi-crystalline polymers.[20]

Patterson's[18] discussion of polymer–solute intermolecular interactions focuses on dispersive and specific interactions between polymer chains and solute molecules. The main contribution of these interactions is toward the enthalpy of mixing, ΔH_M. Dispersion forces and/or random dipole-induced dipole interactions always lead to a positive contribution to ΔH_M and ΔG_M and therefore are not favorable to mixing. In the rarer case of specific interactions, negative contributions to ΔH_M and ΔG_M can result from strong hydrogen bonding forces or charge transfer between polymer and solute molecules.[18]

The free volume effect results from polymer chains having fewer degrees of freedom and more restricted mobility compared to small molecules. This lack of mobility causes polymer chains to have smaller free volumes than small molecules, which have more 'free volume' to wander around their equilibrium positions as they are not tied to an adjacent polymer segment.[20] When polymers and small molecules mix, the polymer's small free volume causes a net contraction in total mixture volume and forces the polymer and solute molecules closer together.[18] This leads to a negative contribution to ΔH_M (favorable to mixing) and a negative contribution to ΔS_M (unfavorable to mixing). These two effects do not cancel out, and the free volume effect leads to a net positive contribution in ΔG_M which is unfavorable for mixing.[18]

A large body of research has been devoted to quantifying these three contributions to polymer–solute mixing by means of the activity coefficient, γ_i. The activity coefficient is related by Equation (2) to the excess Gibbs free energy of mixing, ΔG_M^E, the difference between ΔG_M of a non-ideal system compared with that of its ideal counterpart, ΔG_M^{ideal}. Analogous to ideal small molecule solutions, an ideal polymer–solute solution has equal solute–solute, polymer–solute and polymer–polymer interactions. ΔG_M^{ideal} can be theoretically calculated, with its only contribution being an idealized representation of the combinatorial entropy of mixing:

$$\Delta G_M^E = \Delta G_M - \Delta G_M^{ideal} = RT\sum_i x_i \ln \gamma_i \quad (2)$$

$$\Delta G_M^{ideal} = -T\Delta S_M^{ideal} \quad (3)$$

Conceptually, the activity coefficient provides a measure to account for the deviations from ideality that result from mixing small solute molecules and long polymer chains. The activity coefficient provides a direct indication of polymer–solute affinity, with smaller activity coefficients indicating more favorable mixing. In the case of TPPBs, a polymer or small molecule solvent NAP is best suited for a target molecule when the activity coefficient of the target molecule in the NAP is small. The present work explores the practical benefits of using activity coefficients to quantify polymer–solute affinity, including a convenient approach for experimental activity coefficient evaluation and several easily-accessible prediction methods.

Previous first principles' methods to screen and rank polymer–solute thermodynamic affinity have been limited to analysis of the intermolecular interactions through the use of Hildebrand and Hansen solubility parameters differences.[9,14] Such methods can be effective with polymer solutions due to their significantly lower combinatorial entropy of mixing when compared to small molecules.[21] However, the combinatorial entropy becomes more significant as the molecular weight decreases, as seen in small molecule and oligomeric NAPs, thereby increasing the favorability of mixing by reducing ΔG_M. Due to the significance of molecular weight on ΔG_M, activity models or alternative approaches to predicting polymer–solute affinity can benefit from considering intermolecular interactions, combinatorial entropy and the free volume effect as described above.[16,22,23]

This study uses activity coefficients to characterize the thermodynamic affinity of a polymeric NAP for a range of solutes. A simple and direct correlation between activity coefficients and partition coefficient establishes a framework for polymer screening and evaluation for TPPB applications. The study begins with a demonstration of the influence of solute concentration on partition coefficient for three target molecules specifically selected to possess varying hydrophobicity and aqueous solubility (methyl *tert*-butyl ether, *n*-pentanol, *n*-butyl acetate). Very dilute conditions are shown to be effective for the prediction and experimental evaluation of partition coefficients, with the predictive activity coefficient models demonstrating less precision at higher concentrations.

The use of published infinite dilution activity coefficients is examined for polymer screening applications before evaluating three predictive polymer-phase activity coefficient models for use in cases where literature values are not available. Alternatively, a brief exploration of two surrogate approaches[9,14] to ranking polymer–solute affinity is provided. Both the activity coefficient estimation approach, and the surrogate approaches are evaluated using experimental partition coefficient data collected for 16 solutes (alcohols, ketones, ethers, esters, aromatics) absorbing into poly(*n*-butyl acrylate) at very dilute conditions. This polymer is an amorphous viscoelastic liquid with a glass transition temperature below 25°C ($T_g = -54$°C)[24] that does not present complications associated with crystallinity or an unabsorptive glassy state, thereby isolating polymer–solute thermodynamic affinity.[9,14]

The report concludes with a demonstration of the influence of NAP molecular weight on partition coefficients, highlighting the importance of the combinatorial entropy contribution

towards ΔG_M, and establishing a bridge between small molecule, oligomeric and polymeric TPPB systems. Throughout the work, the activity coefficient based framework for analyzing polymer–solute thermodynamic affinity is discussed in the context of improving polymer NAP screening methods, TPPB processes and operational understanding.

EXPERIMENTAL

Materials and material preparation

All chemicals were purchased from either Sigma-Aldrich (Canada) or Fisher Scientific (Canada). High molecular weight ($M_w \approx$ 100 000 g mol^{-1}) poly(*n*-butyl acrylate) was purchased from Scientific Polymer Products (Ontario, NY) and isolated from toluene solution by solvent evaporation. Low molecular weight ($M_w = 6200$ g mol^{-1}) poly(*n*-butyl acrylate) was prepared by atom transfer radical polymerization (ARGET ATRP) in anisole solution as outlined previously,[25] and purified from residual copper by passing through a silica column before isolating by solvent evaporation.

Partition coefficient tests

Partition coefficient tests were performed in triplicate using three polymer masses, ranging from 0.5 to 1.5 g of dry mass. Each target molecule was prepared in separate aqueous solutions using Type I ultrapure water. In addition to the polymer mass, 10 mL aliquots of aqueous solution were added to each scintillation vial, sealed tightly with a foil lined cap and allowed to equilibrate in an Innova 4400 incubator shaker for 6 days at 30°C and 180 rpm. Aqueous concentrations before and after equilibration were measured using either a Varian 450-GC gas chromatography unit equipped with a CP-8410 AutoInjector, VF-5ms 30 m column and FID detector or a Varian Pro Star HPLC with UV/VIS detection and separated on a Polaris C18 150 × 4.6 mm 5 µm column with a mobile phase of 50:50 water/acetonitrile at 1 mL min^{-1}. A mass balance was performed to determine the solute concentration in the polymer. Experimental partition coefficients were calculated using aqueous and polymer phase weight fractions, w_i^{aq} and w_i^{poly}, in Equation (4). Reported mean and standard deviation (n = 3) values were calculated from triplicate data.

$$\text{Partition Coefficient} = \frac{w_i^{poly}}{w_i^{aq}} \tag{4}$$

RESULTS AND DISCUSSION

Partition coefficient prediction

The partition coefficient is defined as the ratio of the equilibrium solute concentration in the non-aqueous phase (NAP) to that in the aqueous phase. In general, a higher partition coefficient is desired in TPPB applications, as it indicates an increased ability to sequester toxic substrates/products within the NAP. Since phase equilibrium is achieved when a solute's activity is equal in each phase, the partition coefficient can be expressed as a ratio of activity coefficients. Therefore, given appropriate correlations and/or predictions of activity coefficient values for the aqueous phase and the polymeric NAP, partition coefficients can be calculated for any polymer/solute system.

$$a_i^{aq} = a_i^{poly} \tag{5}$$

$$a_i^{\alpha} = \gamma_i^{\alpha} x_i^{\alpha} = \Omega_i^{\alpha} w_i^{\alpha} \tag{6}$$

Therefore

$$\text{Partition Coefficient} = \frac{\Omega_i^{aq}}{\Omega_i^{poly}} \tag{7}$$

where a_i^{α} is the activity, x_i^{α} is the mole fraction, w_i^{α} is the weight fraction, γ_i^{α} is the mole fraction activity coefficient, and Ω_i^{α} is the weight fraction activity coefficient which can be converted from the mole fraction activity coefficient as follows

$$\Omega_i = \gamma_i \frac{x_i}{w_i} \tag{8}$$

Information on the activity of solutes in aqueous solution is widely available, both in terms of experimental data[26–29] and in the form of correlations such as NRTL[30] and UNIQUAC.[31] Where data and correlative model parameters[32] are lacking, fully predictive models such as UNIFAC or modified-UNIFAC may be used to predict activity based on molecular structure. Note that while aqueous-phase activity coefficients are reported on a mole fraction basis, Equation (8) converts them to the weight fraction basis normally used for TPPB systems employing a polymeric NAP.

Compared with aqueous solutions, polymer-phase activity coefficient data are scarce.[33–35] However, there are a number of correlative and fully predictive models available for polymer-phase activity coefficient estimation, several of which have been reviewed by Costa *et al.*[36] Unfortunately, correlative parameters are lacking for the poly(*n*-butyl acrylate) mixtures of present interest, necessitating the use of predictive models such as UNIFAC-vdW-FV [23] and the Flory–Huggins model in conjunction with pure component Hildebrand and Hansen solubility parameters.[21,37]

A simpler approach to gauging polymer–solute affinity which does not involve activity coefficient calculations, utilizes surrogate parameters in their place. Common surrogates include the Hildebrand solubility parameter differences[9,38] and the Hansen 'Ra Distance',[9,21] whose simplicity warrants their use in TPPB polymer screening, but at the expense of thermodynamic rigour.

Effect of solute concentration on partition coefficients

The process of selecting a polymeric NAP for a target molecule often begins with consideration of the solute's published Log $K_{o/w}$ value. This is a measure of the solute's partition coefficient in an *n*-octanol/water system, with high values indicative of a hydrophobic molecule that is best suited to a non-polar NAP. Note that the guidelines for Log $K_{o/w}$ estimation established by the Organization for Economic Co-operation and Development (OECD) require solute concentrations to be <0.01 mol L^{-1} in both the aqueous and *n*-octanol phases.[39] This restriction on solute concentrations ensures that both phases abide by a dilute-ideal solution assumption, and that the system as a whole abides by the Nernst distribution law.[39] The Nernst distribution law states 'the distribution ratio of a solute between two liquid phases at equilibrium is a constant, provided that the solute forms a dilute-ideal solution in each phase.'[40] In a dilute-ideal solution, the solvent approaches ideality and can be represented by Raoult's law ($\gamma_2 \rightarrow 1$) while the solute follows Henry's law ($\gamma_1 \rightarrow \gamma_1^{\infty}$). Therefore, Log $K_{o/w}$ values measured under these conditions are single-point constants that describe solute partitioning under dilute conditions, but they may not reflect the partition coefficient at higher solute concentrations.

Similar arguments pertain to the NAP/water systems of present interest, in that partition coefficients can be concentration dependent, and single-point constants may apply only where both

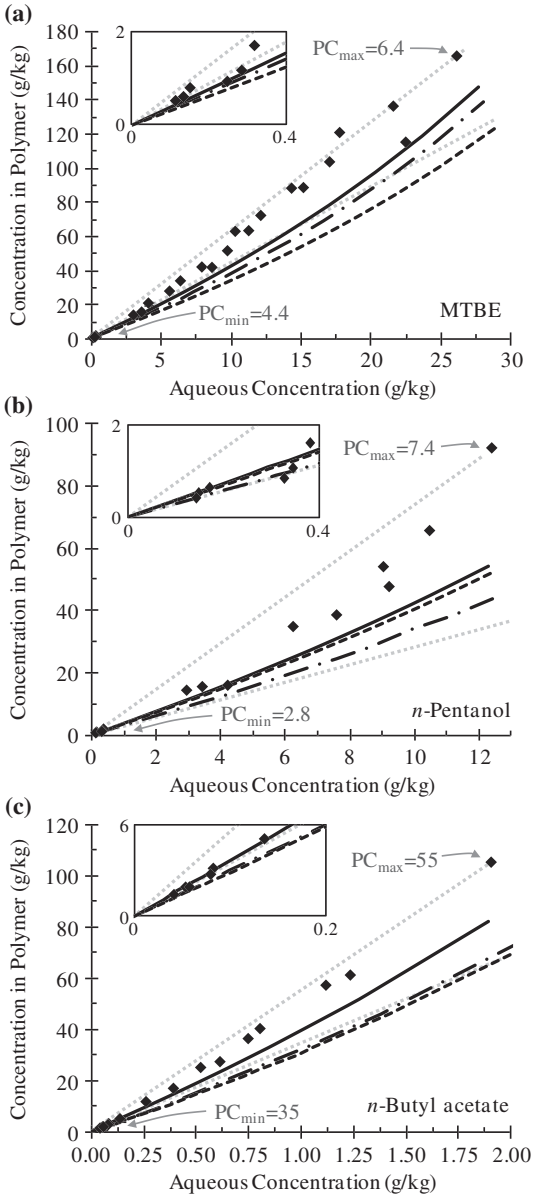

Figure 1. Equilibrium phase composition data (◆) and model predictions for (a) MTBE, (b) *n*-pentanol and (c) *n*-butyl acetate in poly(*n*-butyl acrylate) ($M_w \approx 100\ 000$ g mol^{-1}). Upper and lower bounds of phase composition (.....) are based upon partition coefficient (PC) values at maximum and minimum solute concentration. Inlays show an enlarged view of the very dilute concentration region. Model predictions shown are using UNIFAC-vdW-FV (— · —), FH-HSP (———) and FH-Hildebrand (– – –).

phases abide by a dilute-ideal solution assumption. Consider the data presented in Fig. 1, in which equilibrium MTBE, *n*-pentanol and *n*-butyl acetate concentrations in the aqueous and poly(butyl acrylate) phase are plotted. Using Equation (4), we can identify the ratio of the solute concentration in the polymer (y-axis) to the aqueous concentration (x-axis) as the partition coefficient. Single point partition coefficient (PC) values at minimum and maximum solute concentrations have been extended over the concentration range to form the PC_{min} and PC_{max} lines (.....), illustrating the lower and the upper bounds of experimental phase composition. The upward trends for the experimental data in Fig. 1, from PC_{min} to PC_{max}, suggest that increased equilibrium concentrations correspond to higher partition coefficients, that is, larger ratios of polymer phase to aqueous phase concentrations. The inlays in Fig. 1 show that in the very dilute regime, partition coefficients are nearly constant (i.e. constant slope) and are at the lower PC_{min} boundary. In contrast, partition data at higher concentrations are generally near the upper PC_{max} boundary, indicating higher partition coefficients. The model predictions shown in Fig. 1 are discussed below in the section 'Partition coefficient prediction for non-dilute systems'.

Most partition coefficients for TPPB applications are determined near the inhibitory substrate and/or product concentration,[10,41,42] which may exceed the dilute-ideal solution limit, although this is not always the case.[43] The implications of a concentration-dependent partition coefficient are twofold. In the first place, single-point partition coefficients should be measured and reported at infinitely dilute conditions. Second, recognizing that many TPPB processes operate under conditions that exceed the dilute-ideal solution limit, partition coefficient data should also be provided as a function of solute concentration where these conditions may arise. For example, single phase biodegradation is completely inhibited when exposed to greater than 130 mg L^{-1} of 2,4-dichlorophenol,[10] while ethanol production with *Zymomonas mobilis* is inhibited only when concentrations reach 120 g L^{-1}.[44] Based on the relationships illustrated in Fig. 1, a NAP's absorptive capacity may change during batch fermentation as product concentration increases and/or substrate concentration is reduced. Therefore, TPPB process design requires knowledge of partition coefficient variation with aqueous phase and NAP compositions. However, where the objective is limited to the selection of a polymeric NAP for a given solute, dilute-ideal solution values are likely to suffice.

Evaluation of partition coefficients at infinite dilution

The benefits of infinitely dilute concentrations for initial screening and selection of a polymeric NAP are twofold: (1) partition coefficients can be more easily predicted using single point infinite dilution activity coefficients; and (2) experimental partition coefficients can be analyzed to yield an experimental estimate of the polymer phase activity coefficient.

The first benefit is generally limited to the aqueous phase, for which a wide range of published molar infinite dilution activity coefficients, $\gamma_i^{aq,\infty}$, are available[26–29] and can be converted to the weight fraction activity coefficient using Equation (9). These experimental published values are preferred over predictive or correlative activity models when operating within the infinitely dilute concentration regime. On the other hand, data for polymer-phase activity coefficients, $\Omega_i^{poly,\infty}$, are generally more scarce.[33] For the poly(*n*-butyl acrylate) systems of present interest, polymer phase infinite dilution activity data are unavailable, necessitating the use of activity models to achieve partition coefficient predictions.

$$\Omega_i^{aq,\infty} = \gamma_i^{aq,\infty} \frac{MW_{H2O}}{MW_i} \tag{9}$$

The second benefit of using infinitely dilute conditions arises when evaluating polymer phase activity model predictions. When analyzing a wide range of solutes, each with a unique aqueous activity coefficient, $\Omega_i^{poly,pred}$ cannot be directly compared with experimental partition coefficients. However, experimental partition coefficients can be normalized using the solute's aqueous infinite dilution activity coefficient, $\Omega_i^{aq,\infty}$, to yield an experimental estimate of the polymer phase activity coefficient, $\Omega_i^{poly,expt}$. Thus, a

Table 1. Summary of partition coefficients, experimental polymer phase solute activity coefficients, Hansen Ra and Hildebrand solubility parameter differences, and activity coefficient predictions using Flory–Huggins theory and UNIFAC-vdW-FV. Partition coefficients were determined using poly(*n*-butyl acrylate) ($M_w \approx 100\,000$ g mol^{-1}). Errors shown are +/- one standard deviation

Solute	Partition Coefficient	$\Omega^{aq,\infty}$	$\Omega^{poly,expt}$	Hildebrand $\lvert\Delta\delta\rvert$ (MPa$^{1/2}$)	Hansen 'Ra' Distance (MPa$^{1/2}$)	FH-Hildebrand $\Omega^{poly,pred}$	FH-HSP $\Omega^{poly,pred}$	UNIFAC-vdW-FV $\Omega^{poly,pred}$
Benzene	117 ± 12	538 [d,e,f,g]	4.6 ± 0.7 [c]	0.90	4.94	4.8	4.2	4.0
Toluene	328 ± 66	1806 [d,e,f,g]	5.5 ± 1.1 [c]	0.56	3.71	4.8	3.9	4.1
n-Butanol	0.8 ± 0.4	12.3 [d,e,f,g]	15.4 ± 7.8 [b]	5.59	11.85	15.9	13.0	16.5
n-Pentanol	3.3 ± 0.9	41 [d,e,f,g]	12.5 ± 3.4 [c]	4.32	10.12	11.3	10.8	13.9
n-Hexanol	12 ± 2	134 [d,e,f,g]	11.2 ± 2.1 [c]	3.43	8.79	9.1	9.4	12.3
n-Heptanol	58 ± 4	525 [d,e,f,g]	9.2 ± 1.1 [c]	2.91	7.85	8.1	8.5	11.3
n-Octanol	207 ± 8	1784 [e,f,g]	8.6 ± 0.8 [c]	2.55	7.29	7.5	8.2	10.5
Acetone	0.4 ± 0.2	2.3 [d,e,f,g]	5.8 ± 2.9 [b]	2.33	8.35	6.1	6.2	9.4
Cyclohexanone	3.0 ± 0.4	9.9 [g]	3.3 ± 0.5 [c]	2.73	5.89	5.9	4.4	4.3
Methyl *iso*-butyl ketone	10.6 ± 0.9	53 [f,g]	5.0 ± 0.6 [c]	0.63	4.40	5.2	4.6	6.3
Tetrahydrofuran	1.5 ± 0.3	4.2 [e,f]	2.8 ± 0.6 [b]	1.85	4.56	5.2	3.9	4.4
Methyl *tert*-butyl ether	4.4 ± 0.8	23 [e,f,g]	5.2 ± 1.0 [c]	1.40	4.28	6.1	4.9	5.5
Anisole	208 ± 2	606 [g]	2.9 ± 0.2 [c]	1.98	3.54	4.9	3.4	3.7
Ethyl acetate	2.9 ± 0.3	13 [e,f,g]	4.6 ± 0.6 [b]	0.55	4.20	4.7	3.9	5.3
n-Butyl acetate	35 ± 2	144 [d,e,f,g]	4.1 ± 0.9 [c]	0.20	2.87	4.7	3.7	4.5
iso-Pentyl acetate	113 ± 12	412 [e,f,g]	3.6 ± 0.5 [c]	0.50	3.97	4.8	4.2	4.3

[a] Aqueous phase concentration < 0.01 mol L^{-1} ($\Omega_i^{aq,\infty}$) in all cases.
[b] Polymer phase concentration < 0.01 mol L^{-1} ($\Omega_i^{poly,\infty}$).
[c] Polymer phase concentration < 0.1 mol L^{-1} ($\Omega_i^{poly,expt}$).
Aqueous phase activity references: [d] 26; [e] 27; [f] 28; [g] 29.

direct comparison between experimental and predicted polymer phase activity coefficients is possible.

$$\Omega_i^{poly,expt} = \frac{\Omega_i^{aq,\infty}}{Partition\ Coefficient} \tag{10}$$

The recommended threshold for the accepted dilute-ideal concentration threshold (<0.01 mol L^{-1}) likewise affects the concentration range for which Equation (10) remains valid. For the remainder of this work, partition coefficients were determined at sufficiently dilute conditions such that the aqueous phase concentrations were always <0.01 mol L^{-1}, enabling the use of $\Omega_i^{aq,\infty}$. However, in many cases, particularly when the polymer had a high affinity for the solute, the solute was concentrated in the polymer and exceeded the 0.01 mol L^{-1} limit. In these cases, the experimental polymer phase activity coefficient could not be considered infinitely dilute, $\Omega_i^{poly,\infty}$, and is instead indicated by the experimental equilibrium conditions, $\Omega_i^{poly,expt}$. Table 1 identifies the polymer phase solute concentrations at which the partition data were collected. Efforts were made to obtain partition coefficient data at the lowest possible concentrations, however, analytic detection limits prevented the <0.01 mol L^{-1} condition from holding in some cases.

Estimation of polymer-phase activity coefficients

Activity model identification and implementation

We have examined three polymer-phase activity coefficient models that can be used towards partition coefficient predictions. They include Flory–Huggins solution theory[16] in conjunction with Hildebrand solubility parameters (FH-Hildebrand),[21] Flory–Huggins solution theory in conjunction with Hansen solubility parameters (FH-HSP)[37] and UNIFAC-vdW-FV.[23] The Flory–Huggins solution model[16] considers combinatorial entropy in the first three terms in Equation (11) and by convention, any contribution to ΔG^{mix} which is non-combinatorial (intermolecular interactions and free volume effects) is included in the Flory–Huggins interaction parameter, χ_{12}.[18] A set of sample calculations for the FH-Hildebrand and FH-HSP models is included in the Supporting Information.

$$\ln \gamma_i^{pred} = \underbrace{\ln \frac{\varphi_i}{x_i} + 1 - \frac{\varphi_i}{x_i}}_{combinatorial} + \underbrace{\chi_{ij}\varphi_j^2}_{non-comb} \tag{11}$$

Equation (11) was used to evaluate the mole fraction activity coefficient (γ_i^{pred}) which was subsequently converted to weight fraction activity coefficient ($\Omega_i^{poly,pred}$) using Equation (8).

The use of χ_{ij} is advantageous because binary interaction parameters are specific to the polymer–solute pair of interest. Unfortunately, Flory–Huggins interaction parameters for poly(*n*-butyl acrylate) and the solutes of interest were not available, necessitating the use of the semi-empirical correlations that predict the binary mixture parameter from pure-component data. FH-Hildebrand calculations utilized Equation (12) to provide χ_{ij} estimates from solute and polymer Hildebrand solubility parameters, δ_1 and δ_2. Where V_1 is the molar volume of the solute, and $\beta = 0.34$.[21]

$$\chi_{12} = \frac{V_1}{RT}\left(\delta_1 - \delta_2\right)^2 + \beta \tag{12}$$

Greater insight into the non-combinatorial contributions to polymer–solute mixing can be gained using Hansen solubility parameters to separate the total Hildebrand solubility parameter into three components: atomic dispersion forces (δ_d), polar

dipole–dipole forces (δ_p) and hydrogen bonding interactions (δ_h).[21] FH-HSP calculations were derived from χ_{ij} estimates based on Hansen solubility parameters. The α value is an adjustable parameter which can be used to fit the model to an experimental dataset with sufficient data points, e.g. more than 6.[45] The α parameter was originally prescribed by Lindvig *et al.*[37] to be $\alpha = 0.6$, however, we found that $\alpha = 1.0$ resulted in better predictions for the poly(*n*-butyl acrylate) systems of present interest.

$$\chi_{12} = \alpha \frac{V_1}{RT}\left[\left(\delta_{d1} - \delta_{d2}\right)^2 + 0.25\left(\delta_{p1} - \delta_{p2}\right)^2 + 0.25\left(\delta_{h1} - \delta_{h2}\right)^2\right] \quad (13)$$

In contrast to the Flory–Huggins based models, which use component solubility parameters to quantify polymer–solute interactions, the UNIFAC-vdW-FV model captures how each functional group within the solute molecule and polymer chain interact. Each pair of functional groups present corresponds to an experimentally regressed binary functional group interaction parameter. As outlined by Kannan *et al.*,[23] UNIFAC-vdW-FV is a free volume based activity model akin to the original UNIFAC-FV,[22] that considers combinatorial entropy, intermolecular interactions and free volume effects. The 'UNIFAC-vdW-FV' computer program[46] was used to run calculations with input of polymer and solute molecular structures, bulk densities, polymer molecular weight and solute vapour pressure.

Activity model comparison

Figure 2 presents a comparison of experimental activity coefficient data with predictions derived from the three thermodynamic models. The near 1:1 ratio of predicted vs experimental results (indicated by the dashed line) demonstrates the very good predictability of several solute classes in poly(*n*-butyl acrylate) by all three models. Trends for the primary alcohols (*n*-butanol to *n*-octanol) are most effectively captured by direct activity coefficient estimation methods. It is likely that the parallel structures of the primary alcohols made this series more predictable, whereas the more diverse structures tested within groups such as ethers (THF, MTBE, anisole) or ketones (acetone, MIBK, cyclohexanone) complicated our attempts to predict their phase partitioning behaviour.

The greater thermodynamic rigour employed by considering group contributions in the UNIFAC-vdW-FV model is thought to provide a more fundamental foundation for future polymer screening efforts compared with the semi-empirical correlations relating Hildebrand and Hansen solubility parameters to the Flory–Huggins interaction parameter 'χ_{12}'. However, the Flory–Huggins based models are considerably quicker to compute and may provide adequate results for initial polymer NAP screening for TPPB applications.

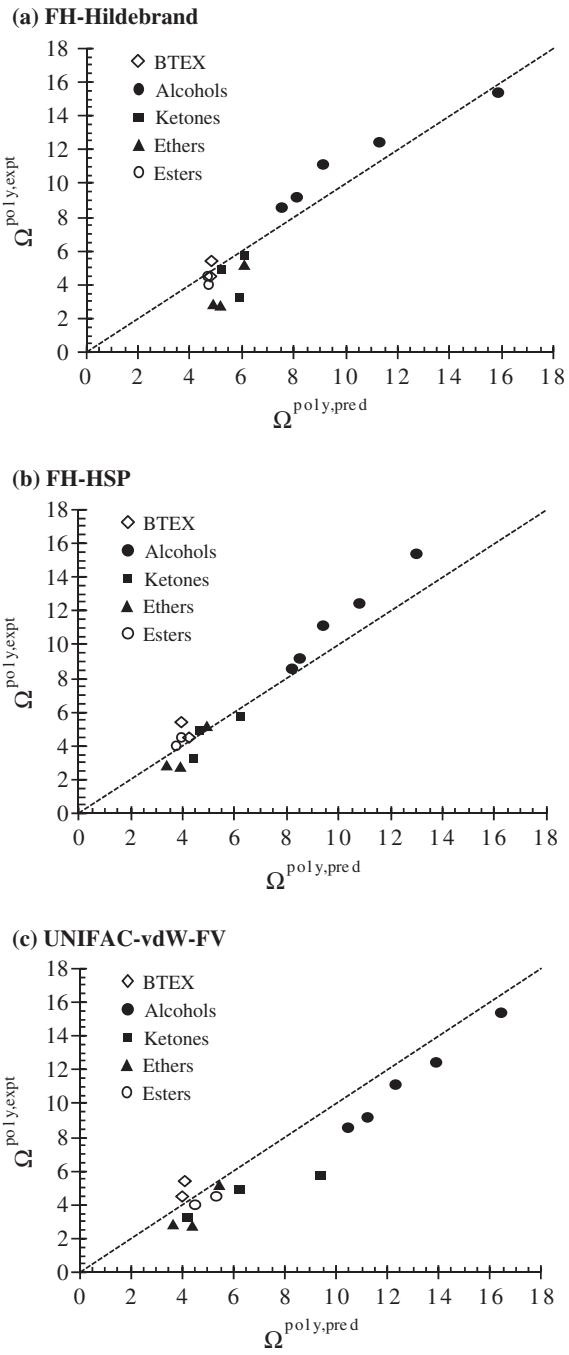

Figure 2. Comparison of weight fraction activity coefficient predictions using (a) FH-Hildebrand, (b) FH-HSP and (c) UNIFAC-vdW-FV with experimental estimates for the weight fraction activity coefficient of various target molecules in poly(*n*-butyl acrylate) ($M_w \approx 100\,000$ g mol^{-1}).

Partition coefficient prediction for non-dilute systems

Equilibrium phase composition predictions using FH-Hildebrand, FH-HSP and UNIFAC-vdW-FV are shown with experimental data in Fig. 1 for MTBE, *n*-pentanol and *n*-butyl acetate in poly(*n*-butyl acrylate). The NRTL model was used to predict the aqueous phase activity coefficient at varying concentrations using experimentally regressed binary model parameters.[32] In accordance with the results in Fig. 2, the three activity models provided good approximations of polymer phase activity coefficients and partition coefficients at very dilute concentrations. However, it is evident in Fig. 1 that the models fail to consider the full effects of phase composition on partition coefficient as the concentrations increase. When compared with the infinitely dilute case in which solute–polymer and polymer–polymer interactions dominate, the additional effect of solute–solute intermolecular interactions at higher concentrations may have contributed to the activity models' poorer precision. These results suggest that the use of these activity models is currently limited to polymer screening applications at infinitely dilute conditions, and that they cannot reliably be used in the place of experimental data to quantify the effects of changing concentrations on TPPB operation.

When predicting partition coefficients for non-dilute systems, activity coefficient evaluation must be performed in conjunction with a system mass balance in an approach equivalent to that of a flash calculation. Contrary to the case in which activity coefficients are fixed at their infinite dilution values, activity coefficients in non-dilute systems vary with composition. In the non-dilute case, an iterative 'flash calculation' approach is required using composition dependent activity models to determine the polymer and aqueous phase concentrations which satisfy the equi-activity requirement in Equation (5).

Surrogate approach to ranking polymer–solute affinity

Two methods of providing a surrogate to polymer–solute thermodynamic affinity were identified as (1) Hildebrand solubility parameter difference and (2) Hansen 'Ra distance'. Hansen solubility parameters used in the 'Ra distance' approach were readily available for all systems using the HSPiP v4.0.04 computer program,[47] which contains a large database of experimental solubility parameter estimates. Compilations of published Hildebrand solubility parameters exist, however for consistency, the Hildebrand solubility parameter was found as the sum of squares of Hansen solubility parameters.

Hildebrand solubility parameter differences

When the difference between a solute's and a polymer's solubility parameters is small, the non-combinatorial contribution to mixing is reduced, resulting in a higher polymer–solute affinity, i.e. a smaller activity coefficient, seen in Fig. 3. Therefore, a simplified surrogate for polymer–solute affinity can be estimated by the Hildebrand solubility parameter difference in Equation (14).

$$|\Delta\delta| = |\delta_{poly} - \delta_{solute}| \tag{14}$$

Hansen 'Ra distance'

The Hansen 'Ra distance' defined in Equation (15) is analogous to the Hildebrand difference, with lower values indicating more favorable mixing between the solute and polymer. The constant '4' before the dispersive parameter produces spherical regions of solubility, thereby simplifying correlations with Hansen solubility parameter differences.[21] A more complete discussion of this corrective constant is available.[21]

$$Ra = \sqrt{4\left(\delta_{d1} - \delta_{d2}\right)^2 + \left(\delta_{p1} - \delta_{p2}\right)^2 + \left(\delta_{h1} - \delta_{h2}\right)^2} \tag{15}$$

Comparison of surrogate approaches

Figure 3 reveals a strong correlation between the experimental infinite dilution polymer-phase activity coefficient and the two surrogate approaches: Hildebrand solubility parameter difference and Hansen 'Ra distance'. The data show that the Hildebrand surrogate approach does not provide a direct (1:1) estimate of activity coefficient, however, a reasonable trend is evident from which a general ranking of polymer–solute affinity can be made. Consistent with a recent report,[9] Fig. 3 indicates that Hansen 'Ra Distance' values provide a more direct (1:1) and linear (R^2) correlation with experimental polymer-phase activity coefficients compared with Hildebrand solubility parameter differences.

By testing a single polymer with a variety of solutes at relatively constant concentration, the combinatorial entropy contribution remains similar between systems. Therefore, Fig. 3 is likely a 'best case' result of the Hildebrand and Hansen surrogate approaches, which does not consider any entropic effects.

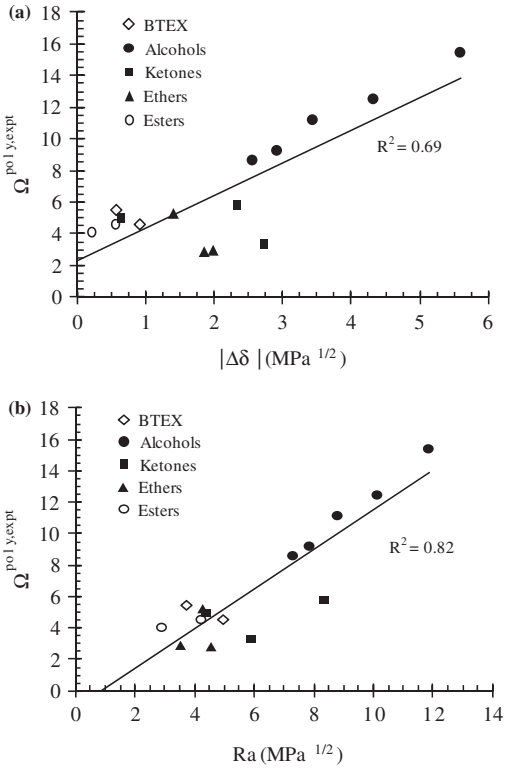

Figure 3. Comparison of (a) absolute Hildebrand solubility parameter difference and (b) Hansen 'Ra distance' with experimental estimates for the weight fraction activity coefficient of various target molecules in poly(*n*-butyl acrylate) ($M_w \approx 100\,000$ g mol^{-1}).

Effect of molecular weight on partition coefficient

Experimental partition coefficients were also measured for solutes from three chemical classes (alcohol, aromatic, ester) absorbing into poly(*n*-butyl acrylate) of two different molecular weights, as well as a representative small molecule (dibutyl adipate). The applicability of dibutyl adipate as a model for low molecular weight poly(*n*-butyl acrylate) was evaluated by comparing activity coefficient predictions for the three solutes in poly(*n*-butyl acrylate) ($M_w = 258$ g mol^{-1}) with those estimated for dibutyl adipate ($M_w = 258$ g mol^{-1}). Differences in polymer–solute activity coefficient predictions varied between the activity model used, with an average absolute deviation for FH-Hildebrand = 1.8%, FH-HSP = 12.6% and UNIFAC-vdW-FV = 3.8%. These comparisons suggest that the composition of dibutyl adipate is a reasonable low molecular weight proxy for our polymer system.

The data listed in Table 2 show that the partition coefficients measured for *n*-butanol, *n*-butyl acetate and benzene increased with decreasing NAP molecular weight. By reducing molecular weight from 100 000 to 258 g mol^{-1}, the partition coefficients increased 85% for benzene, 156% for *n*-butyl acetate and 160% for *n*-butanol. This molecular weight effect was captured by both Flory–Huggins based methods (FH-Hildebrand and FH-HSP) and the UNIFAC-vdW-FV model. A closer analysis of the Flory–Huggins equation (Equation (11)) suggests that the effect of poly(*n*-butyl acrylate) molecular weight is largely captured within the model as an increase in combinatorial entropy. Previous observations on poly(propylene glycol) have also shown molecular weight effects to be significant,[4] as the partition coefficient for *n*-butanol in this system increased from 3.0 to 4.8 as the polymer molecular weight was reduced from 4000 to 1000 g mol^{-1}. Due to the pronounced

Table 2. Comparison of the ability of three activity models to capture the effect of poly(*n*-butyl acrylate) molecular weight on solute activity coefficient in the polymer phase. Aqueous phase infinite dilution activity coefficients were used as reported in Table 1. Errors shown are +/- one standard deviation

Solute	Polymer M_w (g/mol)	Partition Coefficient [c]	$\Omega^{poly,expt}$	FH-Hildebrand $\Omega^{poly,pred}$	FH-HSP $\Omega^{poly,pred}$	UNIFAC-vdW-FV $\Omega^{poly,pred}$
n-Butanol	258 [a]	2.1 ± 0.2	5.9 ± 0.6 [d]	10.5 [b]	6.8 [b]	8.3 [b]
	6,200	1.3 ± 0.1	9.5 ± 0.9 [d]	15.6	12.8	15.9
	100,000	0.8 ± 0.4	15.4 ± 7.8 [d]	15.9	13.0	16.5
n-Butyl Acetate	258 [a]	86 ± 3	1.7 ± 0.4 [e]	2.6 [b]	1.9 [b]	2.0 [b]
	6,200	37 ± 1	3.9 ± 0.8 [e]	4.6	3.6	4.4
	100,000	35 ± 2	4.1 ± 0.9 [e]	4.7	3.7	4.5
Benzene	258 [a]	216 ± 16	2.5 ± 0.3 [e]	3.1 [b]	2.7 [b]	2.2 [b]
	6,200	125 ± 6	4.3 ± 0.5 [e]	4.7	3.7	3.9
	100,000	117 ± 12	4.6 ± 0.7 [e]	4.8	3.8	4.0

[a] Dibutyl adipate (M_w = 258.4 g mol^{-1}) was used as a low molecular weight model compound for poly(*n*-butyl acrylate).
[b] Predictions were made for dibutyl adipate.
[c] Aqueous phase concentration < 0.01 mol L^{-1} ($\Omega_i^{aq,\infty}$) in all cases.
[d] Polymer phase concentration < 0.01 mol L^{-1} ($\Omega_i^{poly,\infty}$).
[e] Polymer phase concentration < 0.1 mol L^{-1} ($\Omega_i^{poly,expt}$).

effect of molecular weight, partition coefficients published in the future will also benefit from reporting the oligomer/polymer molecular weight used.

The effect of molecular weight on the polymer-phase activity coefficient is most pronounced in the low molecular weight region. In some cases lower molecular weight small molecules/oligomers may exhibit operational challenges in TPPBs such as increased foaming,[48] more challenging extractant recovery,[48] and decreased biocompatibility,[4] however, the potential for molecular weight to improve solute partitioning merits further investigation.

A major limitation of the surrogate approaches is that their consideration of polymer–solute affinity cannot capture the combinatorial entropy contribution to mixing. As previously discussed, this contribution is significant in describing how changes in molecular weight affect polymer–solute affinity. Furthermore, in the case of poly(*n*-butyl acrylate), molecular weight has very little effect on Hildebrand and Hansen solubility parameters, and as such, the influence of polymer molecular weight cannot be described by these methods.

CONCLUSIONS

The present study demonstrated that UNIFAC-vdW-FV and Flory–Huggins-based models provide accurate activity coefficient estimates for dilute solutions of small molecule solutes in poly(*n*-butyl acrylate). However, significant deviations between model predictions and experimental activity coefficients were observed at higher solute concentrations, indicating that partition coefficients should be reported along with the solute concentration used to produce the measurement. Furthermore, the sensitivity of partition coefficients to poly(*n*-butyl acrylate) molecular weight was demonstrated experimentally and through thermodynamic modelling, suggesting that partition coefficient values for polymeric systems should be accompanied by molecular weight information.

Supporting Information

Supporting information may be found in the online version of this article.

REFERENCES

1 Daugulis AJ, Swaine DE, Kollerup F and Groom CA, Extractive fermention - integrated reaction and product recovery. *Biotechnol Lett* **9**:425–430 (1987).
2 Daugulis AJ, Partitioning bioreactors. *Curr Opin Biotechnol* **8**:169–174 (1997).
3 Aldric J, Lecomte J and Thonart P, Study on mass transfer of isopropylbenzene and oxygen in a two-phase partitioning bioreactor in the presence of silicone oil. *Appl Biochem Biotechnol* **153**:67–79 (2009).
4 Barton WE and Daugulis AJ, Evaluation of solvents for extractive butanol, fermentation with *Clostridium acetobutylicum* and the use of poly(propylene glycol) 1200. *Appl Microbiol Biotechnol* **36**:632–639 (1992).
5 Fam H and Daugulis AJ, Substrate mass transport in two-phase partitioning bioreactors employing liquid and solid non-aqueous phases. *Bioprocess Biosyst Eng* **35**:1367–1374 (2012).
6 Rehmann L and Daugulis AJ. Biodegradation of PCBs in two-phase partitioning bioreactors following solid extraction from soil. *Biotechnol Bioeng* **99**:1273–1280 (2008).
7 Amsden BG, Bochanysz J and Daugulis AJ, Degradation of xenobiotics in a partitioning bioreactor in which the partitioning phase is a polymer. *Biotechnol Bioeng* **84**:399–405 (2003).
8 Littlejohns JV and Daugulis AJ, A two-phase partitioning airlift bioreactor for the treatment of BTEX contaminated gases. *Biotechnol Bioeng* **103**:1077–1086 (2009).
9 Poleo EE and Daugulis AJ, A comparison of three first principles' methods for predicting solute-polymer affinity, and the simultaneous biodegradation of phenol and butyl acetate in a two-phase partitioning bioreactor. *J Chem Technol Biotechnol* **89**:88–96 (2014).
10 Tomei MC, Annesini MC and Daugulis AJ, 2,4-Dichlorophenol removal in a solid–liquid two phase partitioning bioreactor (TPPB): kinetics of absorption, desorption and biodegradation. *New Biotechnol.* **30**:44–50 (2012).
11 Tomei MC, Annesini MC, Rita S and Daugulis AJ, Two-phase partitioning bioreactors operating with polymers applied to the removal of substituted phenols. *Environ Sci Technol* **44**:7254–7259 (2010).
12 Quijano G, Hernandez M, Thalasso F, Muñoz R and Villaverde S, Two-phase partitioning bioreactors in environmental biotechnology. *Appl Microbiol Biotechnol* **84**:829–946 (2009).
13 Kollerup F and Daugulis AJ, Screening and identification of extractive fermentation solvents using a database. *Can J Chem Eng* **63**:919–927 (1985).
14 Parent JS, Capela M, Dafoe JT and Daugulis AJ, A first principles approach to identifying polymers for use in two-phase partitioning bioreactors. *J Chem Technol Biotechnol* **87**:1059–1065 (2012).

15 Daugulis AJ, Tomei MC and Guieysse B, Overcoming substrate inhibition during biological treatment of monoaromatics: recent advances in bioprocess design. *Appl Microbiol Biotechnol* **90**:1589–1608 (2011).
16 Flory PJ, *Principles of Polymer Chemistry*. Cornell University Press, New York (1953).
17 Patterson D, Role of free volume changes in polymer solution thermodynamics. *J Polym Sci* **16**:3379–3389 (1968).
18 Patterson D, Polymer compatibility with and without a solvent. *Polym Eng Sci* **22**:64–73 (1982).
19 Fredrickson GH, Liu AJ and Bates FS, Entropic corrections to the Flory-Huggins theory of polymer blends: architechtural and conformational effects. *Macromolecules* **27**:2503–2511 (1994).
20 van Dijk MA and Wakker A, *Polymer Thermodynamics Library, Vol. 2: Concepts of Polymer Thermodynamics*. Technomic Publishing Company, Lancaster, PA (1997).
21 Hansen CM. Hansen *Solubility Parameters: A User's Handbook*, 2nd edn. CRC Press, Boca Raton, Fl (2007).
22 Oishi T and Prausnitz JM, Estimation of solvent activities in polymer solutions using a group-contribution method. *Ind Eng Chem Proc Des Dev* **17**:333–339 (1978).
23 Kannan DC, Duda JL and Danner RP, A free-volume term based on the van der Waals partition function for the UNIFAC model. *Fluid Phase Equilibria* **228-229**:321–328 (2005).
24 Brandrup J, Immergut EH and Grulke EA, *Polymer Handbook*, 4th edn. John Wiley & Sons Inc, New York (2003).
25 Payne KA, Cunningham MF and Hutchinson RA, ARGET ATRP of BMA and BA: Exploring Limitations at Low Copper Levels. In *Progress in Controlled Radical Polymerization: Mechanisms and Techniques*, ed by Matyjaszewski K, Sumerlin BS, Tsarevsky NV. American Chemical Society, Washington, DC, 182–202 (2012).
26 Gmehling J, Menke J and Schiller M, *Activity Coefficients at Infinite Dilution*. DECHEMA, Frankfurt (1994).
27 Kojima K, Zhang S and Hiaki T, Measuring methods of infinite dilution activity coefficients and a database for systems including water. *Fluid Phase Equilibria* **141**:145–179 (1997).
28 Estrada E, Díaz GA, Delgado EJ and Estrada E, Predicting infinite dilution activity coefficients of organic compounds in water by quantum-connectivity descriptors. *J Comput Aided Mol Des* **20**:539–548 (2006).
29 Mitchell BE and Jurs PC, Prediction of infinite dilution activity coefficients of organic compounds in aqueous solution from molecular structure. *J Chem Inf Comput Sci* **38**:200–209 (1998).
30 Renon H and Prausnitz JM, Local compositions in thermodynamic excess functions for liquid mixtures. *AIChE* **14**:135–144 (1968).
31 Abrams DS and Prausnitz JM, Statistical thermodynamics of liquid mixtures: a new expression for the excess gibbs energy of partly or completely miscible systems. *AIChE* **21**:116–128 (1975).
32 Arlt W, Macedo MEA, Rasmussen P and Sorensen JM, *Liquid–Liquid Equilibrium Data Collection*. DECHEMA, Frankfurt (1979).
33 Hao W, Elbro HS and Alessi P, *Polymer Solution Data Collection,* Part 2 and 3. DECHEMA, Frankfurt (1992).
34 Orwoll RA and Arnold PA, Polymer–solvent interaction parameter χ, in *Properties of Polymers Handbook*, ed by Mark JE. Physical, Springer, New York, 233–257 (2007).
35 Danner RP and High MS, *Handbook of Polymer Solution Thermodynamics*. American Institute of Chemical Engineers, New York (1993).
36 Costa GMN, Dias T, Cardoso M, Guerrieri Y, Pessoa FLP, Vieira de Melo SAB, *et al.*, Prediction of vapor–liquid and liquid–liquid equilibria for polymer systems: comparison of activity coefficient models. *Fluid Phase Equilibria* **267**(2):140–149 (2008).
37 Lindvig T, Michelsen ML and Kontogeorgis GM, A Flory–Huggins model based on the Hansen solubility parameters. *Fluid Phase Equilibria* **203**:247–260 (2003).
38 Hildebrand J and Scott RL, *The Solubility of Nonelectrolytes*, 3rd edn. Reinhold, New York (1950).
39 OECD, Partition Coefficient (n-octanol/water): Shake Flask Method. OECD Guideline for the Testing of Chemicals. Paris (1995).
40 Marcus Y, Principles of solubility and solutions, in *Solvent Extraction Principles and Practice*, 2nd edn, ed by Rydberg J, Cox M, Musikas C and Choppin GR. Marcel Dekker, Inc., New York, 27–80 (2004).
41 Malinowski JJ and Daugulis AJ, Salt effects in extraction of ethanol, 1 -butanol and acetone from aqueous solutions. *AIChE* **40**:1459–1465 (1994).
42 Nielsen DR, Amarasiriwardena GS and Prather KLJ, Predicting the adsorption of second generation biofuels by polymeric resins with applications for in situ product recovery (ISPR). *Bioresource Technol* **101**:2762–2769 (2010).
43 Tanaka S, Tashiro Y, Kobayashi G, Ikegami T, Negishi H and Sakaki K, Membrane-assisted extractive butanol fermentation by *Clostridium saccharoperbutylacetonicum* N1-4 with 1-dodecanol as the extractant. *Bioresource Technol* **116**:448–452 (2012).
44 Lin Y and Tanaka S, Ethanol fermentation from biomass resources: current state and prospects. *Appl Microbiol Biotechnol* **69**:627–642 (2006).
45 Modarresi H, Conte E, Abildskov J, Gani R and Crafts P, Model-based calculation of solid solubility for solvent selections: a review. *Ind Eng Chem Res* **47**:5234–5242 (2008).
46 Jones A, Kannan D and Danner R, UNIFAC-vdW-FV [Computer program].; 2005 [cited 2013.
47 Abbott S and Yamamoto H, HSPiP [Computer software].; 2013.
48 Quijano G, Hernandez M, Villaverde S, Thalasso F and Muñoz R, A step-forward in the characterization and potential applications of solid and liquid oxygen transfer vectors. *Appl Microbiol Biotechnol* **85**:543–551 (2010).

